Desalination and Water Treatment
www.deswater.com

doi: 10.5004/dwt.2017.21243

85 (2017) 271–281
August

Removal of fluoride and arsenate ions from aqueous solutions and natural water by modified natural materials

G. Vázquez Mejía[a,b], M. Solache-Ríos[a,*], V. Martínez-Miranda[b]

[a]*Instituto Nacional de Investigaciones Nucleares, Depto. de Química, Carretera México Toluca S/N, La Marquesa, Ocoyoacac, México, CP 52750, Tel. +52 5553297200x2271; Fax: +525553297301; emails: marcos.solache@inin.gob.mx (M. Solache-Ríos), gvazquezm@uaemex.mx (G. Vázquez Mejía)*
[b]*Centro Interamericano de Recursos del Agua, Facultad de Ingeniería, Universidad Autónoma del Estado de México, Km. 14.5, carretera Toluca-Atlacomulco, CP 50200, Toluca, Estado de México, México, email: mmirandav@uaemex.mx (V. Martínez-Miranda)*

Received 1 March 2017; Accepted 16 July 2017

ABSTRACT

Fluoride adsorption by modified zeolitic tuff and pozzolana was conducted from aqueous solutions and hot-spring water. The thermodynamic parameters (ΔS, ΔG and ΔH) were calculated from the sorption data obtained at temperatures between 293 and 343 K. Column experiments were carried out using different bed depths; the breakthrough curves obtained for fluoride and arsenic ions from aqueous solutions and natural water were fitted and indicated spontaneous and thermodynamically favorable adsorption for fluoride and arsenic ions by modified zeolitic tuff. The sorption processes of fluoride ions by both adsorbents are endothermic and the mechanisms are physical sorption. The adsorption process of fluoride by modified pozzolana is nonspontaneous, and the sorption of arsenic is endothermic. The highest uptake capacity was obtained with a 3 cm bed depth column and a flow rate of 1 mL/min using a 5 mg/L fluoride solution; the adsorption capacities decreased with the use of hot-spring water.

Keywords: Arsenic; Fluoride; Adsorption; Zeolite; Pozzolan

1. Introduction

Arsenic and fluoride are found naturally in water sources. The correlations between fluoride and arsenic ions in arid and semiarid climates have been studied, mainly in regions with geological characteristics that may favor arsenic and fluoride mobilization into the environment. Fluoride-rich rocks such as fluorspar (CaF_2), cryolite (Na_3AlF_6), fluorapatite ($Ca_5(PO_4)_3F$) and sellaite (MgF_2) are sources of fluoride [1]. Arsenic is found in minerals such as arsenopyrite (FeAsS), realgar (As_2S_2), orpiment (As_2S_3) and arsenic trioxide (As_2O_3) [2]. Arsenic is present as As(III) and As(V) in natural water, depending on the reducing and oxidizing conditions; As(III) is much more toxic than As(V) [3,4].

The World Health Organization recommends maximum limits for drinking water consumption of 0.01 mg As/L and 1.5 mg F^-/L [5]. In some countries such as India, China, Mexico, Argentina and Pakistan, both elements have been found to coexist in some regions [6–10]. The main source of human exposure to these elements is the consumption of contaminated water and food. Fluoride in water causes effects on teeth and bones, known as dental and skeletal fluorosis [11]. Arsenic causes chronic endemic regional hydroarsenicism (HACRE) [12,13]. Exposure to both fluoride and arsenic pollutants causes disorders in the immune systems of children [14].

The coexistence of the fluoride and arsenic ions in groundwater has led to the development of technologies to remove both ions. The adsorption technique is more used than other techniques (coagulation, precipitation, membranes and ion exchange) [15]. Some of the adsorbents used for defluoridation and the removal of

* Corresponding author.

arsenic simultaneously are acid–base treated laterite [16], freshly prepared aluminum hydroxide [17], commercially available hydrated cement, marble powder (waste), brick powder (waste) [18], bone char, goethite-coated sand and hematite-coated sand [19]. There are a few studies in columns about the simultaneous removal of fluoride and arsenic ions. Ruixia et al. [20] tested the removal of fluoride, phosphate and arsenate ions by a modified fiber from water solutions. The aim of this work was to determine the sorption properties of two modified natural materials in batches and continuous systems from water solutions and hot-spring water containing natural excesses of fluoride and arsenic ions; furthermore, the thermodynamic parameters were evaluated in batches.

2. Materials and methods

2.1. Adsorbents and solutions

Pozzolana (PZ) was obtained from Calimaya, Mexico, and zeolitic tuff (ZM) from Oaxaca, Mexico; they were ground and sieved to obtain particles between 16 and 20 meshes. Solutions of fluoride (2–25 mg/L) were prepared from NaF and deionized water, and hot-spring water containing 3.3 mg F^-/L of pH 6.75 was used. Arsenic solutions (0.1–20 mg/L) were prepared from Na_2HAsO_4 (Sigma-Aldrich, Mexico) in deionized water, and natural water from a hot spring containing 4.65 mg As/L was used. The pH of solutions was 6.7 for arsenic and 7.0 for fluoride ions because, in a previous work [21], it was found that these are the best pH values to perform the adsorption experiments.

The materials were modified as reported elsewhere [21]. The pozzolana coated with Fe–Al hydroxides was prepared in two steps. A mixture of Fe–Al hydroxides was prepared by the slow addition of a 2 M KOH solution into a solution containing equal volumes of 0.1 M $FeCl_3$ and 0.1 M $AlCl_3$ solutions under constant stirring (300 rpm) until the pH reached 7.5. The solution was stirred for 30 min; the solid was separated and washed with deionized water to remove the K^+ and Cl^- ions ($AgNO_3$ test). The Fe–Al hydroxides were left with pozzolana in deionized water for 12 h under stirring. Finally, the water was decanted, the coated pozzolana was dried in an oven at 323 K for 5 h and the sample was labeled as PPZ.

The ZM was modified by using an electrochemical process in two steps, iron electrodes were used in the first step and, in the second, aluminum electrodes. The electrode dimensions were 0.1 m long and 0.05 m wide. The electrodes had a total surface area of 0.01 m^2; the direct current power supplied was 3 A at 13 V and had a corresponding a current density of 625 A/m^2. The modification of the material was performed by placing 20 g of ZM in the cell with iron electrodes, 0.4 L of deionized water acidified at pH 2 with concentrated HCl as supporting electrolyte and 2.0 g of NaCl for 1.5 h. Then, the iron electrodes were replaced with aluminum electrodes, and the process was performed in the same conditions for 3 h. Finally, the sample was washed with deionized water until it was free of chloride ions; it was dried in an oven at 323 K for 5 h, and labeled as ZME. Faraday's law was used to calculate the maximum amount of iron and aluminum produced in the electrochemical process.

2.2. Specific surface areas

The Brunauer–Emmett–Teller surface area was obtained by the low temperature N_2 adsorption method (BELSORP-max, Bel, Japan). The samples were heated at 473 K for 2 h before their determinations.

2.3. Fluoride ion determination

The concentration of F^- ions in the solutions was determined with a selective electrode for fluoride ions (Thermo Scientific Orion 4 Star). The total ionic strength adjustment buffer solution (TISAB III) was added to the fluoride standard and samples to control the pH and ionic strength. The calibration curve was obtained by using fluoride standard solutions (1.0–10.0 mg/L).

2.4. Arsenic determination

The concentration of As(V) in the solutions was determined at λ = 193.7 nm through the use of an Atomic Absorption Spectrometer Agilent 200 with a hydride system. The calibration curve was obtained by using arsenic standards solutions (5–20 μg/L).

2.5. Thermodynamic parameters

Batch-type experiments were performed to determine the thermodynamic parameters such as Gibbs free energy (ΔG), enthalpy (ΔH) and entropy (ΔS). Centrifuge tubes with a mixture of 100 mg of sorbent material and 10 mL of fluoride or arsenic solutions (2–25 mg F^-/L or 0.1–20 mg As/L) were shaken at 120 rpm for 2 h at 293, 303, 313, 323 and 343 K. Subsequently, the samples were centrifuged, the liquid phases were decanted and the fluoride and arsenic concentrations were determined by using a selective electrode or atomic absorption spectrometer, respectively.

2.6. Adsorption from binary solutions

Batch sorption from binary solutions containing both elements was performed by using MZE. First, a concentration of 7 mg/L of F^- solution and the concentration of As(V), which was from 0.1 to 1.0 mg/L, were used. In the second test, the concentration of F^- ions varied from 1 to 10 mg/L, and a 1.0 mg/L solution of As(V) was used.

2.7. Sampling and characterization of natural water

The sampling was performed according to the Mexican Official Standard [22], which indicates the procedures for the sampling of water from supply systems for human use and consumption. In Mexico, there are many locations where fluoride ions are present in excess of acceptable limits (>1.5 mg F/L and >0.01 mg As/L) in natural water [23]. A hot-spring water sample was collected and characterized; the electrical conductivity, pH, acidity, alkalinity, total hardness, chlorides, sulfates, nitrates, fluorides, potassium, sodium, iron and arsenic were determined by using standard methods [24].

2.8. Continuous system

The accumulation of fluoride and arsenic in a fixed-bed column is dependent on the quantity of the adsorbent in the column. The adsorption process was performed in columns of a 15 mm internal diameter, and they were loaded with 1, 2 and 3 g of MZE; the heights of the beds were 1, 1.5 and 2.2 cm, respectively. The solution and natural water were eluted at a constant volumetric flow rate of 1 mL/min, and the fluoride concentrations were 5.0 and 3.3 mg F^-/L for the solution and hot-spring water, respectively. For arsenic, the columns were loaded with 0.5 and 1.0 g of MZE, and the heights of the beds were 0.5 and 1.0 cm, respectively. The solution and natural water were eluted at a constant volumetric flow rate of 1 mL/min, and the arsenic concentrations were 2.0 and 4.65 mg of As(V)/L for the solution and hot-spring water, respectively. The breakthrough curves were obtained by plotting the ratio of C_e/C_0 (C_e and C_0 are the fluoride or arsenic concentrations of effluents and influents, respectively) against time.

3. Results and discussion

3.1. Characterization of the materials

The characterization of the adsorbents by X-ray diffraction, scanning electron microscopy with energy X-ray disperse spectroscopy analysis and the points of zero charge (pH_{zpc}) were reported elsewhere [21]. Oxygen, sodium, aluminum, silicon, potassium, iron and calcium were found in the samples. Aluminum and iron increased considerably after the treatment of the materials (12% for aluminum in the zeolitic material and 15% for iron in pozzolana). The diffractograms of natural and modified zeolitic materials corresponded mainly to sodium aluminum silicate hydrate, clinoptilolite, cristobalite alpha and moganite. The diffractograms showed that the pozzolana samples contained mainly cordierite, anorthoclase, anorthite, sodium aluminum silicate and calcium aluminum silicate. The pH_{pzc} for the iron–aluminum modified zeolite and pozzolana (ZME and PPZ) was 6.7 for both materials [21].

The surface area of the electrochemically modified zeolite (72.84 m^2/g) was higher than that of the natural material (14.36 m^2/g). These values are similar to those reported by Macedo-Miranda [25]: 10.77 and 11.10 m^2/g for two zeolites. Teutli-Sequeira et al. [26] modified a natural zeolite using aluminum electrodes, obtaining a surface area of 39.56 m^2/g. The surface area of the zeolite increased by about 50% after the modification by an electrochemical process. The specific surface area of the modified pozzolana (6.36 m^2/g) was higher than that of the natural material (1.60 m^2/g).

3.2. Adsorption isotherms of fluoride and arsenic ions at different temperatures

The data obtained at different temperatures were treated with the adsorption models of Langmuir, Langmuir–Freundlich and Freundlich, and the results were best fitted to the last one by using the software Origin 8. The constants K_F and n of the Freundlich model were calculated from the intercept and slope of the linear plot of $\log q_e$ vs. $\log C_e$, respectively. K_F is defined as the Freundlich adsorption coefficient, which is proportional to the adsorption capacities for fluoride or arsenic ions. The Freundlich constant, $1/n$, provides information about the adsorption intensity or surface heterogeneity [27].

3.2.1. Fluoride

The adsorption parameters calculated from the experimental data and Freundlich model are summarized in Table 1. The main trend observed is that fluoride ions adsorption by MZE and PPZ increased with the increasing temperature (Fig. 1), which is in agreement with the results reported from the use of other adsorbents [28,29]. The values of $1/n$ are in a range of 0.31–0.37 for the case of MZE-F at temperatures of 293, 303 and

Table 1
Adsorption isotherms parameters of fluoride and arsenic ions by MZE and PPZ

Freundlich model $q_e = K_f \times C_e^{1/n}$					
Temperature (K)		MZE-F	PPZ-F	MZE-As	PPZ-As
293	K_F (mg/g) (L/mg)	0.64	0.33	1.16	6.24
	$1/n$	0.31	0.31	0.67	0.66
	R^2	0.99	0.94	0.98	0.93
303	K_F (mg/g) (L/mg)	0.64	0.06	1.54	1.08
	$1/n$	0.39	0.65	0.72	0.55
	R^2	0.96	0.75	0.95	0.98
313	K_F (mg/g) (L/mg)	0.70	0.03	3.98	0.30
	$1/n$	0.37	0.87	1.09	0.7
	R^2	0.96	0.96	0.99	0.73
323	K_F (mg/g) (L/mg)	1.12	0.07	–	7.54
	$1/n$	0.20	0.69	–	1.63
	R^2	0.81	0.77	–	0.98
343	K_F (mg/g) (L/mg)	1.15	0.089	–	–
	$1/n$	0.86	0.82	–	–
	R^2	0.95	0.95	–	–

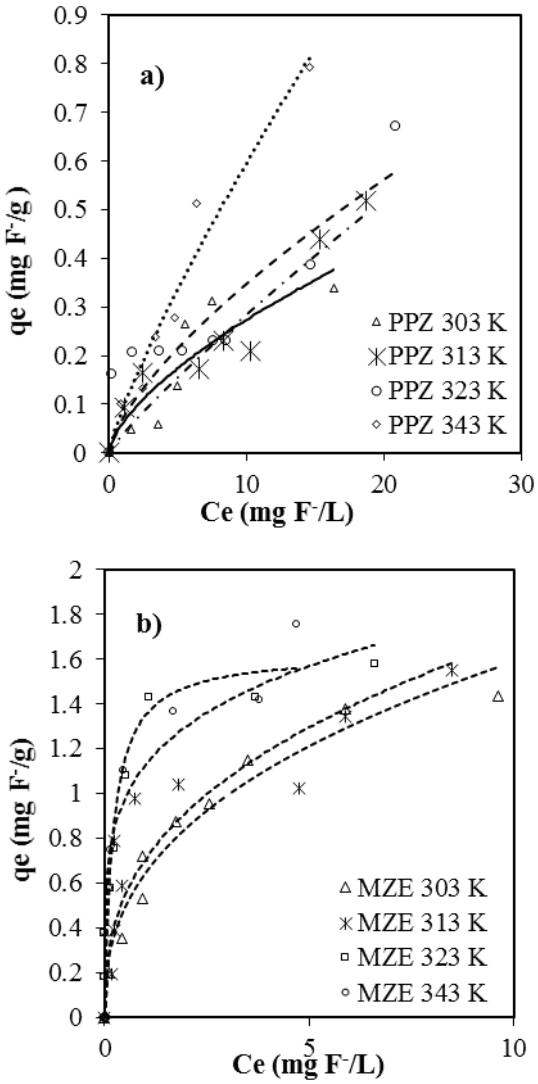

Fig. 1. Adsorption isotherms of F^- by PPZ (a) and MZE (b) at 303, 313, 323 and 343 K fitted to Freundlich model.

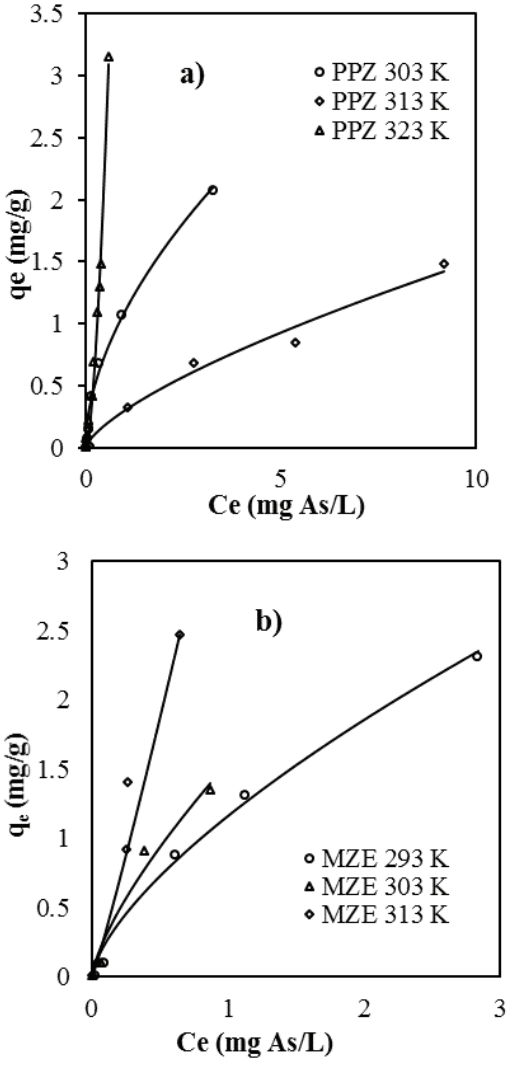

Fig. 2. Adsorption isotherms of As(V) by PPZ (a) at 303, 313 and 323 K; MZE (b) at 293, 303 and 313 K fitted to Freundlich model.

313 K. At a higher temperature (323 K), it decreased to 0.20, indicating a higher interaction of the solute and the adsorbent; however, at 343 K, the interaction decreased ($1/n$ = 0.86). The value of $1/n$ obtained at 293 K for PPZ-F reflects a good interaction between the fluoride ion and the adsorbent; however, at a higher temperature, the interaction decreases.

3.2.2. Arsenic

Fig. 2(a) shows the adsorption isotherms of As(V) by PPZ. The adsorption capacity decreases with the increasing temperature; similar results have been observed for diatomite coated with iron oxide [30]. Fig. 2(b) shows that the adsorption of As(V) by MZE increased with increasing temperature. The experimental data fit reasonably well with the Freundlich model. The K_F and $1/n$ values are highest for the adsorption of arsenic at 313 K (7.54 mg/g and 1.63, respectively). The values of $1/n$ (Table 1) suggest a weak adsorption interaction of As and MZE or PPZ, which decreases with the increasing temperature.

3.3. Thermodynamic parameters for the adsorption processes of fluoride and arsenic ions

The thermodynamic parameters including free energy (ΔG), enthalpy (ΔH) and entropy (ΔS) for the adsorption processes were determined from the slopes (K_d) of the adsorption isotherms (Figs. 1 and 2) at different temperatures. ΔH and ΔS were calculated from the plot of $\ln(K_d)$ vs. $1/T$ and the Van't Hoff equation (Eq. (1)); this was performed for the fluoride and arsenic ions [31]:

$$\ln K_d = -\frac{\Delta \mathrm{H}}{R}\left(\frac{1}{T}\right) + \frac{\Delta S}{R} \tag{1}$$

where R is the universal constant of ideal gases (8.314 J/mol K) and T is the temperature in Kelvin. The free energies of activation (ΔG) at different temperatures were calculated by Eq. 2 [32]:

$$\Delta G = \Delta H - T\Delta S \tag{2}$$

3.3.1. Fluoride

The equations obtained for the fluoride ions from the plot of $\ln K_d$ vs. $1/T$ were $\ln K_d = -5{,}206\ (1/K) + 16.844$ and $\ln K_d = -2{,}100.9\ (1/K) + 3.154$ for MZE and PPZ, respectively. The positive ΔH (kJ/mol) values (Table 2) indicate the endothermic processes of fluoride adsorption by MZE and PPZ. The positive entropy changes (ΔS) obtained for the systems of fluoride solutions on MZE and PPZ indicate a high degree of randomness in the solid/liquid interface. On the other hand, the positive values of ΔS (Table 2) suggest that the freedom of the fluoride ions is not restricted by the adsorbents, confirming physical adsorption [15].

The positive values of ΔG (kJ/mol) (Table 2) indicate the nonspontaneous nature of the fluoride adsorption reaction with MZE at 303 K and with PPZ at all temperatures studied, which shows that the sorption mechanism may be chemisorption. Moreover, the free energy of the process was found to decrease with the increasing temperature. The negative values of ΔG at 313–343 K suggest that the adsorption of fluoride by MZE is spontaneous and that MZE has a high affinity for fluoride ions from the solution under the experimental conditions.

Table 2
Thermodynamic parameters for the adsorption of fluoride and As(V) ions by MZE and PPZ

Parameter		Fluoride solution		Arsenic solution	
		MZE-F	PPZ-F	MZE-As	PPZ-As
ΔH (kJ/mol)		43.28	17.46	65.49	–151.46
ΔS (J/mol)		140.04	26.22	205.37	–491.87
ΔG (kJ/mol)	T (K)	ΔG	ΔG	ΔG	ΔG
	293	–	–	–	–7.346
	303	0.850	9.521	–	–2.427
	313	–5.501	9.259	1.206	2.490
	323	–1.950	8.997	–8.475	–
	343	–4.751	8.473	–4.955	–

3.3.2. Arsenic

The equations obtained for the arsenic ions from the plot of $\ln K_d$ vs. $1/T$ were $\ln K_d = -7{,}876.8(1/K) + 24.702$ and $\ln K_d = 18{,}218(1/K) - 59.162$ for MZE and PPZ, respectively. The positive value of ΔH shows an endothermic adsorption behavior of As(V) by MZE. The absolute magnitude of the heat of physisorption usually changes from 2 to 30 kJ/mol. It is also known that the heat of physisorption is typically about 10 kJ/mol. However, the enthalpy change due to chemisorption generally falls in the range of 40–200 kJ/mol, which is larger than that of physisorption. Because of the calculated values for ΔH in this work, the adsorption of As(V) onto MZE is attributed to a chemisorption phenomenon. Further, the positive value of ΔS denotes an increment of randomness at the solid–liquid interface during the adsorption process [30]. The negative values of ΔG in Table 2 suggest that the As(V) adsorption by MZE is spontaneous and is favorable at higher temperatures. However, the positive ΔG value at 313 K indicates that spontaneity is not favored.

The negative value of the standard entropy, ΔS, suggests that randomness decreases at the solid/solution interface during the sorption of arsenic ions by PPZ. The negative value of ΔH again indicates the exothermic nature of the adsorption process. The change in free energy is used to determine the spontaneity of the adsorption reaction, and the higher negative value of ΔG indicates thermodynamically favorable adsorption. The negative values of ΔG suggest that the As(V) adsorption by PPZ is spontaneous and is favorable at higher temperatures.

Table 3 shows the thermodynamic parameters of the adsorption processes of fluoride and arsenic ions with the different adsorbents materials reported in the literature. Most studies on the adsorption of fluoride ions show negative values of ΔG, as it was found for the zeolitic material in this work. Negative values indicate a good affinity of F^- ions for the adsorbent and spontaneous adsorption processes. The pozzolana

Table 3
Thermodynamic parameter for fluoride and arsenic ions by different adsorbents

Adsorbent	ΔG (KJ mol^{-1})	Temperature (K)			ΔH (KJ mol^{-1})	ΔS (J mol^{-1} K^{-1})	Reference
Fluoride							
Al–Fe modified zeolite	0.85 (303)	–5.50 (313)	–1.95 (323)	–4.75 (343)	43.24	140.04	Present study
Al–Fe modified pozzolan	9.52 (303)	9.25 (313)	8.99 (323)	8.47 (343)	17.46	26.22	Present study
Iron(III)–tin(IV) mixed oxide	2.32 (283)	2.19 (298)	2.06 (313)	1.93 (328)	4.79	8.72	[33]
Alkoxide origin alumina	–4.26 (293)	–2.98 (313)	–2.52 (323)	–	–0.059	–59.1	[34]
Surfactant-modified pumice	–2.5 (293)	–2.63 (298)	2.92 (303)	–	4.422	23.2	[35]
Aluminum-modified zeolite	–3.05 (303)	–3.51 (313)	–3.97 (323)	–	10.91	46.02	[36]
Arsenic							
Al–Fe modified zeolite	1.20 (313)	–8.47 (323)	–4.95 (343)	–	65.49	205.37	Present study
Al–Fe modified pozzolan	–7.34 (293)	–2.42 (303)	2.49 (313)	–	–151.4	–491.87	Present study
Dolomite	80.57 (293)	87.75 (318)	93.50 (338)	–	–3.67	–287.35	[37]
Feldspars	A: 1.07 (288)	–0.66 (298)	–2.32 (308)	–	50	170	[31]
	B: 0.38 (288)	–0.20 (298)	–0.94 (308)		19.3	65.7	
Granular ferric hydroxide	–2.71 (293)	–3.19 (303)	–3.65 (313)	–	10.98	–	[38]

studied in this work presents positive values of ΔG; the same behavior was reported by Biswas et al. [33], who employed an iron(III)–tin(IV) mixed oxide. The positive ΔG values (Table 3) indicate the nonspontaneous adsorption reaction of fluoride. All studies have shown positive ΔH values except for the F^- adsorption by alkoxide origin alumina at temperatures of 293–323K [34]. The ΔS values were mostly positive, indicating a strong affinity of F^- toward the adsorbents.

The negative and positive values of ΔG of adsorption of arsenic indicate spontaneous and nonspontaneous processes, respectively, and it depends on the temperature. Most studies on adsorption of arsenic resulted in positive values of ΔH which suggest the endothermic nature of adsorption, except for arsenic adsorption by pozzolana (present study) and dolomite [37] as they have negative values and suggest exothermic processes. The ΔS values were mostly positive in this study, indicating again a strong affinity of arsenic toward the adsorbents.

3.4. Adsorption of fluoride and arsenic from the binary solutions

Fig. 3 shows the removal percentage of As(V) vs. F^-. The removal of As(V) ranged between 96% and 98% whereas the removal of F^- varied between 84% and 87%. Generally, it was observed that the adsorption of both anions is similar in single and binary solutions. Fig. 4(a) shows the adsorption of the F^- ions isotherm data fitted to Freundlich model in the presence of arsenic (1 mg As/L). The parameters calculated from the model are K_F = 0.972, n = 4.34 and R^2 = 0.811; the experimental adsorption capacity was 0.76 mg F^-/g MZE.

The Freundlich adsorption isotherm of As(V) by MZE in the presence of fluoride ions (7 mg F^-/L) is shown in Fig. 4(b). The parameters calculated from the model are K_F = 0.462, n = 2.36 and R^2 = 0.842. The maximum experimental adsorption capacity is 0.07 mg As(V)/g MZE. The results suggest that MZE can be used as an adsorbent of fluoride and arsenic ions.

3.5. Adsorption of fluoride and arsenic ions from a hot-spring water sample

3.5.1. Characterization of hot-spring water

Table 4 shows the characterization of the hot-spring water used in the experiments. The concentrations of fluoride and arsenic ions are higher than the limits allowed by the World Health Organization guidelines. The pH of the hot-spring water was 6.7, which is acceptable; the recommended pH values are between 6.5 and 8.5 for hot-spring water. Chloride and sodium occur naturally in hot-spring water; the concentrations of chloride and sodium were 998.2 and 873.05 mg/L, respectively. These elements did not significantly affect the process of the adsorption of fluoride and arsenic ions by MZE.

3.5.2. Isotherms

Fig. 5(a) shows the adsorption capacities for fluoride ions vs. the quantity of the adsorbents in the hot-spring water. The adsorption capacity decreases as the dose of the adsorbent (MZE) increases. A dose of 100 mg/10 mL is sufficient to reduce the concentration to the permissible levels established

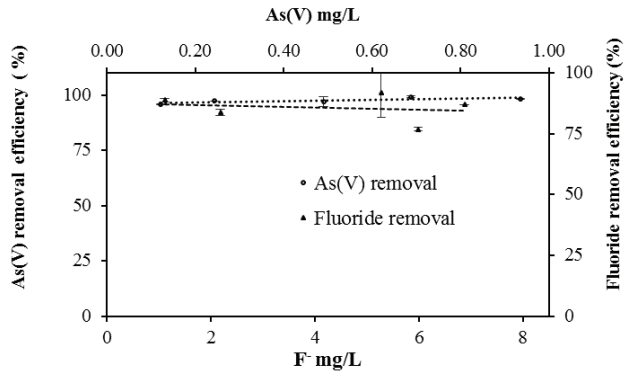

Fig. 3. Arsenic and fluoride removal by MZE in the presence of fluoride solutions at concentrations from 1.0 to 8.0 mg/L and the presence of As(V) solutions at concentrations from 0.1 to 0.8 mg/L.

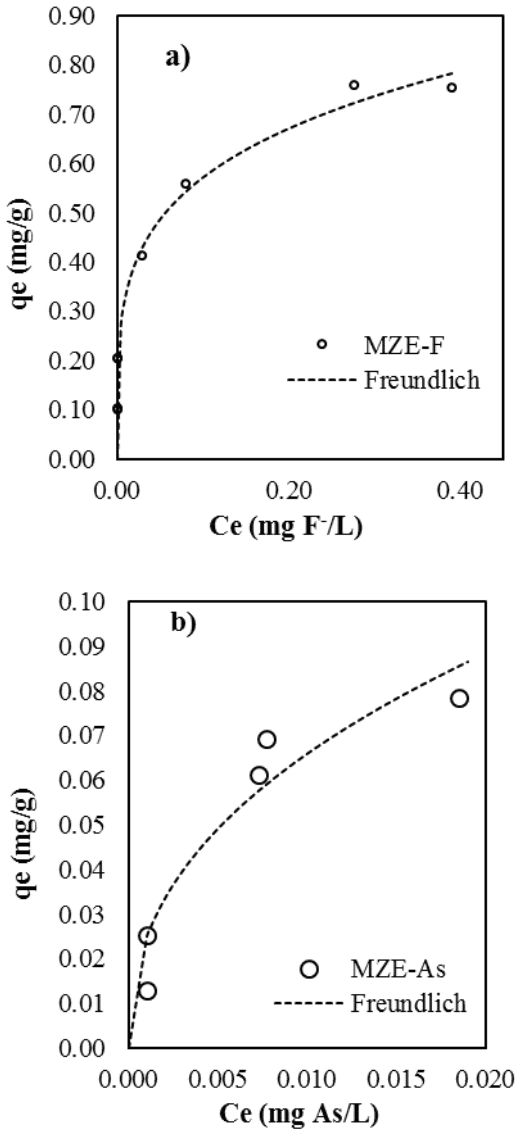

Fig. 4. (a) Adsorption isotherm F^- ions by MZE with initial concentration of As(V) solution = 1 mg As/L; pH = 6.06–6.45, contact time = 24 h. (b) Adsorption isotherm As(V) by MZE with the presence of fluoride ions (7 mg/L); pH = 6, contact time = 24 h.

Table 4
Characterization of hot-spring water

Parameter	Value	[5]
Temperature	70°C (in situ)	
pH	6.75	6.5–8.5
Electrical conductivity	3.375 mS/cm	
Acidity	85.49 mg/L $CaCO_3$	
Alkalinity	136.62 mg/L $CaCO_3$	
Chloride	998.20 mg/L Cl^-	250 mg/L Cl^-
Total hardness	92.36 mg/L $CaCO_3$	500 mg/L $CaCO_3$
Ca hardness	36.62 mg/L $CaCO_3$	
Sulfates	186.84 mg/L SO_4^{2-}	400 mg/L SO_4^{2-}
Potassium	45.52 mg/L K	
Sodium	873.05 mg/L Na	200 mg/Na
Iron	<0.1 mg/L Fe	0.30 mg/L Fe
Nitrates	<0.01 mg/L NO_3^-	
Fluorides	3.3 mg/L F^-	1.5 mg/L F^-
Arsenic	4.65 mg/L As	0.01 mg/L As

by the WHO. It is important to highlight that even though the concentration of Cl^- ions is high, its interference is insignificant on the F^- removal.

The adsorption isotherm of fluoride ions from hot-spring water by MZE were adjusted to the Freundlich model, and the parameters obtained are K_F = 0.264 (mg/g) (L/mg), $1/n$ = 0.056 and R^2 = 0.827 (Fig. 6). The Freundlich, K_F, equilibrium is proportional to the adsorption capacity and the reciprocal of n; the lower values of these two constants in hot-spring water compared with those obtained with the aqueous solutions (K_F = 0.64 (mg/g) (L/mg), $1/n$ = 0.13, R^2 = 0.99) is mainly due to the presence of other ions in the hot-spring water. A similar effect was observed by Teutli-Sequeira et al. [26] using an aluminum-modified zeolite and natural water containing 8.29 mg F^-/L.

Fig. 5(b) shows the adsorption capacity of MZE for arsenic vs. the mass of the adsorbent in the hot-spring water. The arsenic adsorption capacity decreases as the mass of the adsorbent increases; the same behavior was observed for fluoride ions. Additionally, 92% removal was obtained using 150 mg of material.

3.5.3. Column systems

3.5.3.1. Fluoride The breakthrough point was taken as 1.5 mg/L, which is the maximum limit established by the World Health Organization [5]. The adsorbed pollutant at breakpoint (q_b) was obtained from the following equation [39]:

$$q_b = \frac{Q_v t_b C_0}{m_c} \quad (3)$$

where t_b is the service time at the breakpoint, C_0 is the inlet ion concentration (mg/L), Q_v is the effluent volumetric flow rate (L/min) and m_c is the amount of adsorbent (g). The adsorption bed capacities of the column up to the breakpoint were 0.41, 0.76 and 1.96 mg/g for 1, 2 and 3 g of MZE, respectively. The breakthrough times were 74, 270 and 1,280 min for bed depths of 1, 1.5 and 2.2 cm of MZE, respectively. The breakthrough increased as the mass of MZE increased using an aqueous solution of 5 mg F^-/L.

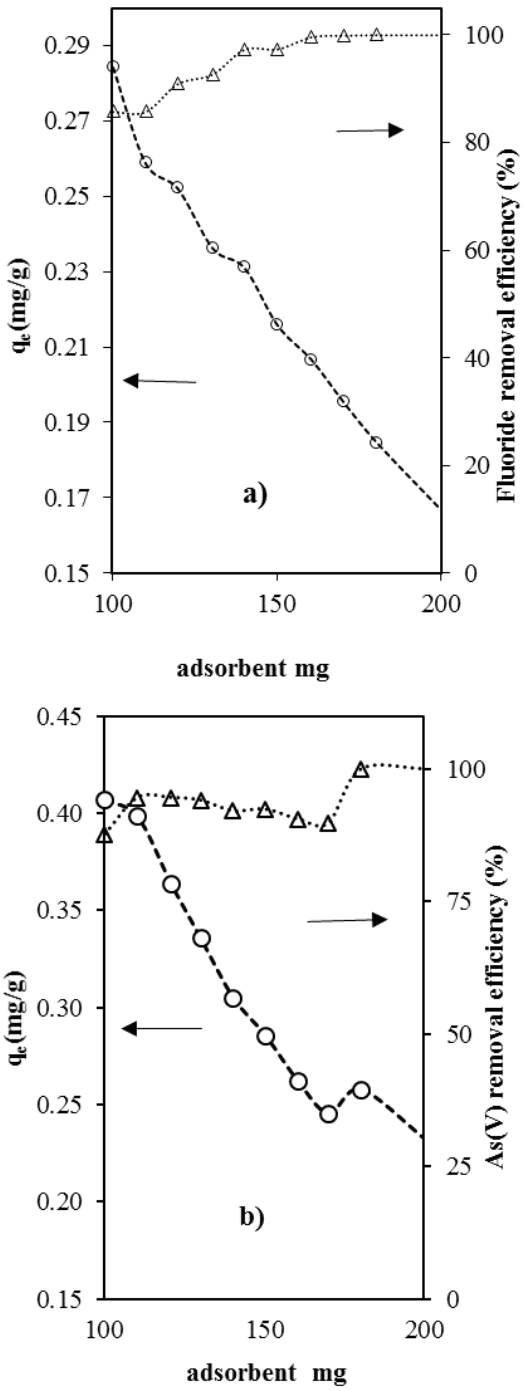

Fig. 5. (a) Effect of adsorbent dose on adsorption of fluoride onto MZE from hot-spring water (concentration = 3.3 mg F^-/L, pH = 6.75, contact time = 24 h). (b) Effect of adsorbent dose on adsorption of As(V) onto MZE from hot-spring water (concentration 3.3 mg F^-/L, pH = 6.75, contact time = 24 h).

The adsorption capacities of the columns up to the breakpoint were 0.11 and 0.19 mg/g for 0.5 and 1 g of MZE,

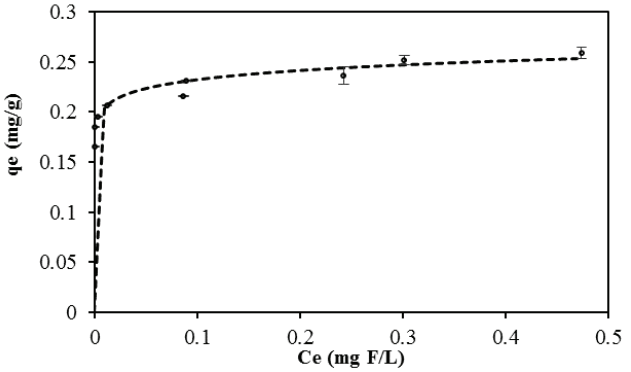

Fig. 6. Freundlich isotherm of fluoride ions by MZE from hot-spring water (concentration = 3.3 mg F^-/L, pH = 6.75, contact time = 24 h).

respectively, using hot-spring water (3.3 mg F^-/L). The breakthrough times were 15 and 55 min for bed depths of 0.5 and 1.0 cm of MZE, respectively. The composition of the hot-spring water may be responsible for the decrease of the adsorption capacities.

3.5.3.2. Arsenic The adsorption bed capacities of the column up to the breakpoint for As(V) by MZE were calculated by Eq. (3), and the values were 0.02 and 0.01 mg/g for 0.5 and 1.0 g of adsorbent, respectively. The service time at breakpoint when the outlet concentration was 0.01 mg/L (which is the maximum limit established by the World Health Organization [5]) was reached in approximately 5 min.

3.5.3.3. Thomas and Bohart–Adams models Mathematical models have been reported to describe and possibly predict the dynamic behavior of the solute in a column [40]. The experimental data were fitted to the Thomas and Bohart–Adams models by the help of the software Origin 8.0. The Bohart–Adams model was applied to the adsorption kinetics data until the breakpoint was reached; the Thomas model was also applied to the adsorption kinetics data until saturation was reached.

The model assumes that the adsorption rate is proportional to both the residual capacity of the adsorbent material and the concentration of the solute species, which is mainly determined by the adsorbent surface sites, and it is used to describe the initial part of the breakthrough curve. In accordance with the Bohart–Adams model, Eq. (4) is used to predict the performance of the continuous adsorption columns [41]:

$$\frac{C}{C_0}\exp\left(k_{AB}C_0t - k_{AB}N_0\frac{Z}{F}\right) \quad (4)$$

where N_0 is the saturation concentration (mg/L), K_{AB} is the kinetic constant (L/mg min), Z is the bed depth of column (cm) and v is the linear flow rate (cm/min). The equation $v = Q/A$ was used to calculate the linear flow rate where A is the transversal area of the column (cm^2) and Q is the volumetric flow (mL/min).

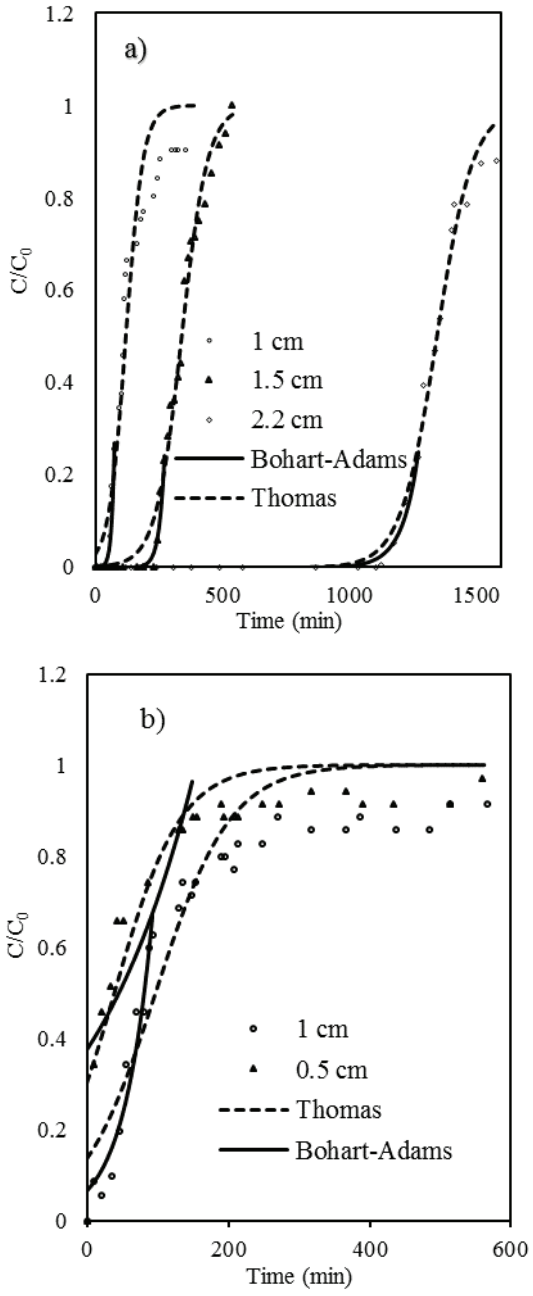

Fig. 7. Breakthrough curves of fluoride ions by MZE using fluoride solutions (a) and hot-spring water (b) in columns of different bed depth adjusted to Thomas and Adams–Bohart models.

3.5.3.4. Fluoride This approach was applied to all breakthrough curves using a nonlinear regression analysis (Fig. 7) for aqueous solutions and hot-spring water. The relative values of K_{AB} and N_0 were calculated (Table 5), and the values of R^2 were between 0.88 and 0.97. In general, the values of K_{AB} decreased as the bed depth increased whereas N_0 increases with increase in the bed height for the aqueous solution, and for hot-spring water, an opposite behavior was observed. The data from hot-spring water using 0.5 g of MZE could not be adjusted to the Bohart–Adams model.

Table 5
Bohart–Adams model parameters for adsorption of F^- ions on MZE (initial concentration 10 and 3.3 mg F^-/L for solutions and hot-spring water, respectively)

Bed depth (cm)	M (g)	Aqueous solution			Bed depth (cm)	M (g)	Hot spring water		
		K_{BA} (L/mg min)	N_0 (mg/L)	R^2			K_{BA} (L/mg min)	N_0 (mg/L)	R^2
MZE-F					MZE-F				
1	1	0.01667	275.632	0.88	0.5	0.5	0.00182	604.944	0.66
1.5	2	0.00864	624.744	0.95	1.0	1.0	0.00708	213.711	0.93
2.2	3	0.0034	1593.41	0.97					

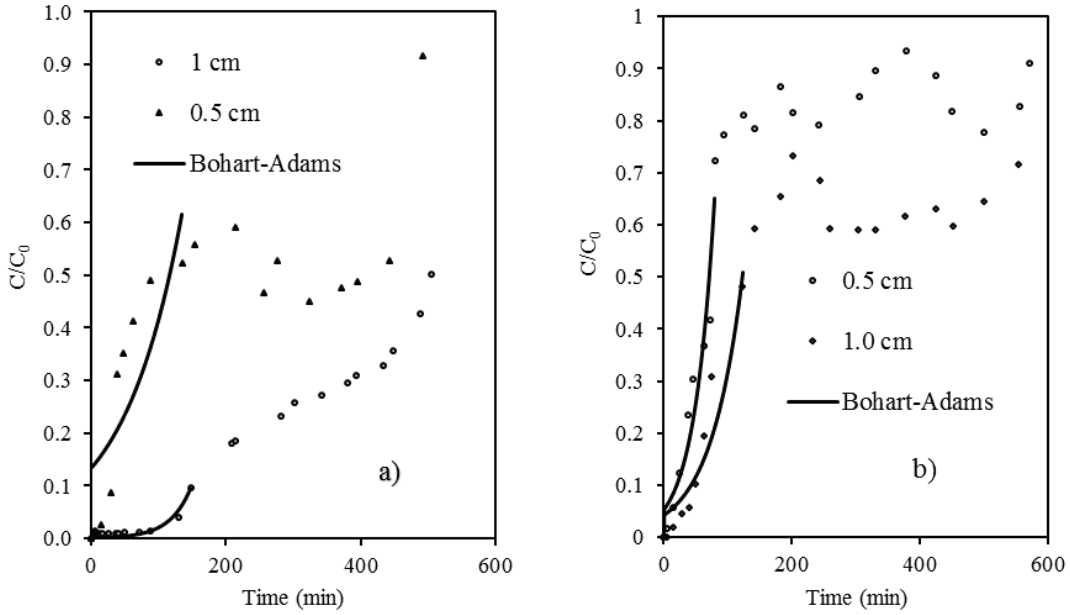

Fig. 8. Breakthrough curves of As(V) by MZE using arsenic solutions (a) and hot-spring water (b) in columns of different bed depths adjusted to Bohart–Adams model.

3.5.3.5. Arsenic Fig. 8 shows the breakthrough curves of the adsorption of arsenic by MZE with water solutions and hot-spring water. The relative values of K_{AB} and N_0 were calculated and shown in Table 6, and the values of R^2 were between 0.87 and 0.92 for hot-spring water. The data from the aqueous solution with 0.5 g of MZE could not be adjusted to the model (R^2 was low). In general, the values of K_{AB} and N_0 decreased as the bed depth increased.

3.5.3.6. Thomas model The maximum adsorption capacity of an adsorbent can be calculated with the Thomas model [42]. This model predicts breakthrough curves under different experimental conditions. The equation of the Thomas model is:

$$\frac{C_e}{C_0} = \frac{1}{1+\exp\left[\dfrac{K_{TH}}{Q(q_0 M - C_0 V)}\right]} \quad (5)$$

where C_e is the effluent fluoride concentration (mg/L), C_0 is the influent fluoride concentration (mg/L), K_{TH} is the rate constant (L/mg h), Q is the volumetric flow rate through column (L/h), q_0 is the total sorption capacity (mg/g), V is the throughput volume (L) and M is the mass of the adsorbent (g). The experimental results were adjusted to this model using fluoride solutions and hot-spring water (Fig. 8), and the parameters determined for the breakthrough curves are given in Table 7. The values of the kinetic constant, K_{TH}, decreases, and the adsorption capacity, q_0, increases with increases in the bed heights, which indicates that the mass transport resistance increases for MZE. It was also observed that the q_0 values calculated from the Thomas model are similar to the experimental values (0.41, 0.76 and 1.96 mg/g for 1, 2 and 3 g, respectively).

Mechanisms on the adsorption of arsenic by an aluminosilicate modified with iron(III) have been reported by Macedo-Miranda [25]. The adsorption of arsenic by these materials may take place by an ionic exchange of the arsenic chemical species with hydroxyl groups or by the formation of bidentate complexes with iron(III).

The proposed adsorption mechanism of fluoride ions by aluminum and iron-modified materials is mainly by an ion exchange of hydroxyl ions with fluoride ions [15].

Table 6
Bohart–Adams model parameters for adsorption of As(V) on MZE (initial concentration 2 and 4.65 mg As(V)/L for solution and hot-spring water, respectively)

Bed depth (cm)	M (g)	Aqueous solution			Bed depth (cm)	M (g)	Hot-spring water		
		K_{BA} (L/mg min)	N_0 (mg/L)	R^2			K_{BA} (L/mg min)	N_0 (mg/L)	R^2
MZEAs					MZEAs				
0.5	0.5	0.0056	400.85	0.595	0.5	0.5	0.0066	494.83	0.9217
1	1	0.0153	259.89	0.9167	1.0	1.0	0.0043	412.48	0.8759

Table 7
Thomas model parameters for adsorption of F^- ions on MZE (initial concentration 10 and 3.3 mg F^-/L for solution and hot-spring water, respectively)

Bed depth (cm)	M (g)	Aqueous solution			Bed depth (cm)	M (g)	Hot-spring water		
		K_{TH} (L/mg min)	q_0 (mg/g)	R^2			K_{TH} (L/mg min)	q_0 (mg/g)	R^2
MZE-F					MZE-F				
1	1	0.00531	0.672	0.910	0.5	0.5	0.0102	0.0818	0.8379
1.5	2	0.00349	0.952	0.986	1.0	1.0	0.0090	0.2036	0.878
2.2	3	0.00304	2.062	0.988	–	–	–	–	–

4. Conclusions

The thermodynamic parameters ΔH and ΔS suggest that the adsorption processes of F^- by both materials are endothermic with a high degree of randomness and that the adsorption process for As(V) ions by PPZ is exothermic. Free energy values, ΔG, indicate a spontaneous process for the adsorption of F^- ions by MZE and As(V) by both materials. The ΔG values indicate a nonspontaneous process for the adsorption of F^- ions by PPZ.

The removal of the F^- and As(V) ions present in hot-spring water was carried out efficiently by MZE. The dose of the adsorbent positively affected the adsorption of these ions. The presence of Cl^- ions in hot-spring water did not affect the removal of fluoride.

The sorption behaviors of fluoride and arsenic ions by MZE from aqueous solutions and hot-spring water were determined in a continuous flow. Fluoride ion uptake and breakthrough times increased as the bed heights increased.

The Thomas model was also used to predict the breakthrough curves under varying bed depths; this model was fitted to the processes of the adsorption of the fluoride ions in aqueous solutions and hot-spring water. This model resulted in good agreement between the experimental and calculated breakthrough curves. The Thomas rate constant (K_T) and the maximum adsorption capacity (q_0) increased with increases in the bed height.

The modified MZE zeolite is a potential adsorbent for the removal of F^- ions and As(V) from water solutions and hot-spring water.

Acknowledgments

The authors are very thankful to Dr. Ma. Teresa Olguín for her support to do this work. The authors acknowledge a scholarship grant from COMECYT No. 13BCD0030-II for GVM and the authors are grateful to CONACYT for the financial support, project 254665.

References

[1] S.V. Jadhav, E. Bringas, G.D. Yadav, V.K. Rathod, I. Ortiz, K.V. Marathe, Arsenic and fluoride contaminated groundwaters: a review of current technologies for contaminants removal, J. Environ. Manage., 162 (2015) 306–325.
[2] P.L. Smedley, D.G. Kinniburgh, A review of the source, behaviour and distribution of arsenic in natural waters, Appl. Geochem., 17 (2002) 517–568.
[3] V.K. Sharma, M. Sohn, Aquatic arsenic: toxicity, speciation, transformations, and remediation, Environ. Int., 35 (2009) 743–759.
[4] J. Bundschuh, M.I. Litter, F. Parvez, G. Román-Ross, H.B. Nicolli, J.S. Jean, C.-H. Liu, D. López, M.A. Armienta, L.R.G. Guilherme, A. Gómez Cuevas, L. Cornejo, L. Cumbal, R. Toujaguez, One century of arsenic exposure in Latin America: a review of history and occurrence from 14 countries, Sci. Total Environ., 429 (2012) 2–35.
[5] Guidelines for Drinking Water Quality, WHO, Geneva, 2011.
[6] R. Indu, S. Krishnan, T. Shah, Impacts of groundwater contamination with fluoride and arsenic, Int. J. Rural Manage., 3 (2007) 69–93.
[7] D. Wen, F. Zhang, E. Zhang, C. Wang, S. Han, Y. Zheng, Arsenic, fluoride and iodine in groundwater of China, J. Geochem. Explor., 135 (2013) 1–21.
[8] M.A. Armienta, N. Segovia, Arsenic and fluoride in the groundwater of Mexico, Environ. Geochem. Health., 30 (2008) 345.
[9] M.L. Gomez, M.T. Blarasin, D.E. Martínez, Arsenic and fluoride in a loess aquifer in the central area of Argentina, Environ Geol., 57 (2009)143–155.
[10] S.J. Mahmood, N. Taj, F. Parveen, T.H. Usmani, R. Azmat, F. Uddin, Arsenic, fluoride and nitrate in drinking water: the problem and its possible solution, Res. J. Environ. Sci., 1 (2007) 179–184.
[11] M. Mohapatra, S. Anand, B.K. Mishra, D.E. Giles, P. Singh, Review of fluoride removal from drinking water, J. Environ. Manage., 91 (2009) 67–77.
[12] G. Sun, Arsenic contamination and arsenicosis in China, Toxicol. Appl. Pharmacol., 198 (2004) 268–271.
[13] A.A. Duker, E.J.M. Carranza, M. Hale, Arsenic geochemistry and health, Environ. Int., 31 (2005) 631–641.
[14] B.L. Estrada-Capetillo, M.D. Ortíz-Pérez, M. Salgado-Bustamante, E. Calderón-Aranda, C.J. Rodríguez-Pinal, E. Reynaga-Hernández, N.E. Corral-Fernández,

R. González-Amaro, D.P. Portalez-Pérez, Arsenic and fluoride co-exposure affects the expression of apoptotic and inflammatory genes and proteins in mononuclear cells from children, Mutat. Res./Genet. Toxicol. Environ. Mutagen., 761 (2014) 27–34.
[15] P. Loganathan, S. Vigneswaran, J. Kandasamy, R. Naidu, Defluoridation of drinking water using adsorption processes, J. Hazard. Mater., 248–249 (2013) 1–19.
[16] V.K. Rathore, D.K. Dohare, P. Mondal, Competitive adsorption between arsenic and fluoride from binary mixture on chemically treated laterite, J. Environ. Chem. Eng., 4 (2016) 2417–2430.
[17] R. Liu, Simultaneous removal of arsenic and fluoride by freshly-prepared aluminum hydroxide, Colloids Surf., A, 466 (2015) 147–153.
[18] S. Bibi, A. Farooqi, K. Hussain, N. Haider, Evaluation of industrial based adsorbents for simultaneous removal of arsenic and fluoride from drinking water, J. Cleaner Prod., 87 (2015) 882–896.
[19] T.B. Mlilo, L.R. Brunson, D.A. Sabatini, Arsenic and fluoride removal using simple materials, J. Environ. Eng., 136 (2010) 391–398.
[20] L. Ruixia, G. Jinlong, T. Hongxiao, Adsorption of fluoride, phosphate, and arsenate ions on a new type of ion exchange fiber, J. Colloid Interface Sci., 248 (2002) 268–274.
[21] G. Vázquez Mejía, V. Martínez-Miranda, C. Fall, I. Linares-Hernández, M. Solache-Ríos, Comparison of Fe–Al-modified natural materials by an electrochemical method and chemical precipitation for the adsorption of F^- and As(V), Environ. Technol., 37 (2016) 558–568.
[22] NOM, Mexicana, Diario Oficial de la Federación, 2000.
[23] M.T. Alarcón-Herrera, J. Bundschuh, B. Nath, H.B. Nicolli, M. Gutiérrez, V.M. Reyes-Gómez, D. Núñez, I.R. Martín-Domínguez, O. Sracek, Co-occurrence of arsenic and fluoride in groundwater of semi-arid regions in Latin America: genesis, mobility and remediation, J. Hazard. Mater., 262 (2013) 960–969.
[24] A.D. Eaton, L.S. Clesceri, A.E. Greenberg, M.A.H. Franson, American Public Health Association, American Water Works Association, Water Environment Federation, Standard Methods for the Examination of Water and Wastewater, American Public Health Association, Washington, D.C., 2005.
[25] G. Macedo-Miranda, Evaluación del proceso de sorción de la clonoptilolita natural mexicana para el tratamiento de aguas contaminadas con arsénico, Instituto Tecnológico de Toluca, Tesis doctoral, Toluca, México, 2007.
[26] A. Teutli-Sequeira, M. Solache-Ríos, V. Martínez-Miranda, I. Linares-Hernández, Comparison of aluminum modified natural materials in the removal of fluoride ions, J. Colloid Interface Sci., 418 (2014) 254–260.
[27] B.-S. Zhu, Y. Jia, Z. Jin, B. Sun, T. Luo, X.-Y. Yu, L.-T. Kong, X.-J. Huang, J.-H. Liu, Controlled synthesis of natroalunite microtubes and spheres with excellent fluoride removal performance, Chem. Eng. J., 271 (2015) 240–251.
[28] Y. Zhang, X. Lin, Q. Zhou, X. Luo, Fluoride adsorption from aqueous solution by magnetic core-shell Fe_3O_4@alginate-La particles fabricated via electro-coextrusion, Appl. Surf. Sci., 389 (2016) 34–45.
[29] W.-X. Gong, J.-H. Qu, R.-P. Liu, H.-C. Lan, Adsorption of fluoride onto different types of aluminas, Chem. Eng. J., 189–190 (2012) 126–133.
[30] Y.-F. Pan, C.T. Chiou, T.-F. Lin, Adsorption of arsenic(V) by iron-oxide-coated diatomite (IOCD), Environ. Sci. Pollut. Res., 17 (2010) 1401–1410.
[31] M. Yazdani, T. Tuutijärvi, A. Bhatnagar, R. Vahala, Adsorptive removal of arsenic(V) from aqueous phase by feldspars: kinetics, mechanism, and thermodynamic aspects of adsorption, J. Mol. Liq., 214 (2016) 149–156.
[32] R. Chang, E.J.H.D. Bourneville, Quimica, Editorial McGraw-Hill, 2007.
[33] K. Biswas, K. Gupta, U.C. Ghosh, Adsorption of fluoride by hydrous iron(III)–tin(IV) bimetal mixed oxide from the aqueous solutions, Chem. Eng. J., 149 (2009) 196–206.
[34] S.P. Kamble, G. Deshpande, P.P. Barve, S. Rayalu, N.K. Labhsetwar, A. Malyshew, B.D. Kulkarni, Adsorption of fluoride from aqueous solution by alumina of alkoxide nature: batch and continuous operation, Desalination, 264 (2010) 15–23.
[35] G. Asgari, B. Roshani, G. Ghanizadeh, The investigation of kinetic and isotherm of fluoride adsorption onto functionalize pumice stone, J. Hazard. Mater., 217–218 (2012) 123–132.
[36] A. Teutli-Sequeira, M. Solache-Ríos, V. Martínez-Miranda, I. Linares-Hernández, Behavior of fluoride removal by aluminum modified zeolitic tuff and hematite in column systems and the thermodynamic parameters of the process, Water Air Soil Pollut., 226 (2015) 239.
[37] Y. Salameh, N. Al-Lagtah, M.N.M. Ahmad, S.J. Allen, G.M. Walker, Kinetic and thermodynamic investigations on arsenic adsorption onto dolomitic sorbents, Chem. Eng. J., 160 (2010) 440–446.
[38] K. Banerjee, G.L, Amy, M. Prevost, S. Nour, M. Jekel, P.M. Gallagher, C.D. Blumenschein, Kinetic and thermodynamic aspects of adsorption of arsenic onto granular ferric hydroxide (GFH), Water Res., 42 (2008) 3371–3378.
[39] V.C. Taty-Costodes, H. Fauduet, C. Porte, Y.-S. Ho, Removal of lead (II) ions from synthetic and real effluents using immobilized *Pinus sylvestris* sawdust: adsorption on a fixed-bed column, J. Hazard. Mater., 123 (2005) 135–144.
[40] M. Trgo, N.V. Medvidović, J. Perić, Application of mathematical empirical models to dynamic removal of lead on natural zeolite clinoptilolite in a fixed bed column, Indian J. Chem. Technol., 18 (2011) 123–131.
[41] G.S. Bohart, E.Q. Adams, Some aspects of the behavior of charcoal with respect to chlorine.1, J. Am. Chem. Soc., 42 (1920) 523–544.
[42] H.C. Thomas, Heterogeneous ion exchange in a flowing system, J. Am. Chem. Soc., 66 (1944) 1664–1666.